Proceedings of Meetings on Acoustics

Volume 59 http://acousticalsociety.org/

23rd International Symposium on Nonlinear Acoustics

Nanjing, China
30 June - 4 July 2025

Physical Acoustics

Analysis of nonlinear propagation and shock formation in high-intensity focused ultrasound from a multi-element array in air

Oleg A. Sapozhnikov, Shamil A. Asfandiyarov, Anastasiya V. Lapina, Sergey A. Tsysar and Petr V. Yuldashev

Lomonosov Moscow State University Faculty of Physics: Moskovskij gosudarstvennyj universitet imeni M V Lomonosova Fiziceskij fakul'tet; Moscow, 119991, RUSSIAN FEDERATION; oa.sapozhnikov@gmail.com; shoma.ufa@gmail.com; lapinaav@my.msu.ru; sergey@acs366.phys.msu.ru; petr@acs366.phys.msu.ru

A multi-element ultrasound array for generating high-intensity focused ultrasound (HIFU) in air in the low-frequency ultrasonic range has been developed and manufactured. The array elements are 128 piezoelectric transducers mounted on a spherical base with the ability to adjust their position. The operating frequency is 35.5 kHz, the source diameter and focal length are 0.5 m. The elements are installed close to each other, and their centers are located on 8 spirals to avoid periodicity and thereby suppress parasitic diffraction maxima. All array elements are electrically connected in parallel and excited by a signal from a power amplifier. To study the characteristics of the emitted ultrasound beam, the transient acoustic holography method was used. Nonlinear propagation effects in the focused beam were modeled using the «HIFU beam» free software. It was shown experimentally and theoretically that the waveform at the focus of the developed array contains developed shock fronts, and the maximum achievable peak positive acoustic pressure level exceeds 175 dB.

Proceedings of Meetings on Acoustics, Vol. 59, 045001 (2025); https://doi.org/10.1121/2.0002215.

1. INTRODUCTION

Ultrasound sources operating in the megahertz range are extensively employed in medical therapeutic applications.[1] By focusing ultrasound in liquids and biological tissues, it is possible to generate extremely high acoustic pressures, reaching 100 – 150 MPa, which are critical for thermally or mechanically disrupting targeted regions of biological tissue within the human body.[2] These high-intensity focused ultrasound (HIFU) fields routinely produce shocked, sawtooth-like waveforms at the focus, characterized by steep shock fronts and broad harmonic spectra.

In contrast, HIFU transducers designed for air environments have not yet seen widespread development or diverse applications. To attain elevated acoustic pressure levels, low-frequency ultrasonic systems have been engineered, relying on piezoceramic transducers, such as Langevin vibrators, paired with large, contoured radiating plates.[3] These airborne ultrasonic systems are applied in industrial processes, including defoaming, drying fruits and vegetables, deactivating microorganisms, and enhancing various processes in gaseous environments.[4, 5] Research indicates that these systems, when operating in a focused mode, can achieve pressure levels up to 175 dB.[3] While effective for their intended purposes, these devices struggle to achieve precise localization of high-intensity zones to form acoustic fields with specific desired configurations.

Drawing inspiration from medical HIFU applications, high-intensity focused fields can be generated in air using multielement antenna arrays. These arrays enable independent adjustment of the amplitudes and phases of signals from individual elements, offering versatile control over the emitted wave field's structure. Additionally, research in this direction has demonstrated the use of focused ultrasound for acoustic levitation in air, enabling the manipulation, suspension, and rotation of small objects, such as polystyrene spheres and tiny liquid droplets weighing a few milligrams.[6, 7, 8] In high-intensity operating conditions, nonlinear acoustic phenomena play a critical role, making them highly relevant for numerous applications.[9, 10, 11]

The objective of this study was to leverage a previously developed 128-element ultrasonic focusing array [12] to generate a low-frequency ultrasound beam in air with sufficient intensity to produce a shocked waveform at the focal point, mirroring the behavior observed in HIFU beams used in liquids and biological tissues for advanced therapeutic systems.

2. MATERIALS AND METHODS

A. THEORETICAL ANALYSIS OF THE SIMILARITY BETWEEN HIFU MODES IN THERAPEUTIC SYSTEMS AND LOW-FREQUENCY ULTRASOUND SOURCES IN AIR

The Westervelt equation, which describes the combined effects of nonlinearity, diffraction, and dissipation in finite-amplitude acoustic waves, is given by [13]

$$\Delta p - \frac{1}{c_0^2}\frac{\partial^2 p}{\partial t^2} = -\frac{\beta}{\rho_0 c_0^4}\frac{\partial^2 (p^2)}{\partial t^2} + \hat{L}(p)\,,$$

where p is the acoustic pressure, t is time, $\Delta = \partial^2/\partial x^2 + \partial^2/\partial y^2 + \partial^2/\partial z^2$ is the Laplacian, c_0 is the small-signal speed of sound, ρ_0 is the ambient density, β is the coefficient of acoustic nonlinearity, and $\hat{L}(p)$ is linear intergo-differential operator that accounts for dissipation and dispersion in the medium. In a classical thermoviscous fluid, the dissipation operator takes the simple local form $\hat{L}(p) = -\frac{\delta}{c_0^4}\frac{\partial^3 p}{\partial t^3}$, where δ is the sound diffusivity (or effective dissipation

coefficient). In more complex media such as biological tissues or air, the operator $\hat{L}(p)$ generally has a different, often frequency-dependent form that incorporates relaxation processes.

Consider an acoustic source operating at frequency f. Normalize spatial coordinates by the wavenumber $k = 2\pi/\lambda$, where λ is the wavelength $\lambda = c_0/f$: $\mathbf{R} = k\mathbf{r}$, where $\mathbf{r} = (x, y, z)$. The dimensionless Laplacian is then $\tilde{\Delta} = k^{-2}\Delta$. Introduce dimensionless time $\theta = \omega\tau$ with $\omega = 2\pi f$ and normalize pressure by characteristic "internal" medium pressure $p_* = \rho_0 c_0^2/\beta$: $P = p/p_*$. The Westervelt equation then transforms to the dimensionless form

$$\tilde{\Delta}P - \frac{\partial^2 P}{\partial\theta^2} = -\Gamma\frac{\partial^3 P}{\partial\theta^3} - \frac{\partial^2(P^2)}{\partial\theta^2} + \hat{\Lambda}(P) \ .$$

Here the operator $\hat{\Lambda}(P) \sim \hat{L}(p)$ accounts for linear absorption and dispersion. In many practical situations the attenuation can be neglected. For instance, low-frequency ultrasound propagating in air and megahertz range ultrasound propagating in water are characterized by the absorption length of several tenths of meters.[14, 15] Consequently, when investigating the acoustic field at sub-meter distances from the source, the corresponding attenuation term in the Westervelt equation can be omitted without significant loss of accuracy:

$$\tilde{\Delta}P - \frac{\partial^2(P - P^2)}{\partial\theta^2} = 0 \ .$$

The wave equation in such a form does not contain any medium-specific parameter. Nonlinear and diffraction phenomena in acoustic beams from different sources and media are therefore identical provided (*i*) source geometrical parameters measured in wavelengths are equal and (*ii*) surface pressure amplitudes p_0 normalized by the medium's internal pressure p_* , p_0/p_* , are equal.

This similarity implies that a megahertz-range HIFU beam in water or tissue matches a beam from a larger source in air when D/λ, F/λ, and $\beta\, p_0/(\rho_0 c_0^2)$ are identical, where D is the source diameter, F is the focal length, and p_0 is the source pressure amplitude. For example, consider an airborne source with $D = F = 0.5$ m and f=35.5 kHz. Here λ=9.66 mm, yielding $D/\lambda = F/\lambda =$ 51.7. Medium parameters are ρ_0=1.205 kg/m^3, c_0 =343 m/s, $\beta = 1.2$, so $p_* = \rho_0 c_0^2/\beta =$ 0.118 MPa . A matching waterborne source (ρ_0=998 kg/m^3, c_0 =1481 m/s, $\beta = 3.5$) at f=1 MHz has λ=1.48 mm and thus $D = F = 7.66$ cm to preserve D/λ and F/λ. Such dimensions are typical of therapeutic HIFU transducers.[1] The characteristic pressure in air is 5300 times lower than in water (for which p_* =625 MPa), requiring source pressures in air to be correspondingly lower for equivalent nonlinear effects. Studies of megahertz HIFU in water show that sources with diameter and focal length of several centimeters exhibit strongly nonlinear behavior when p_0 > 0.5 MPa, producing shocked focal waveforms.[16] By similarity, shocked waveforms in air are expected for p_0 > 100 Pa levels achievable with the experimental system of Ref. 12 employed here.

B. NUMERICAL SIMULATION

Simulations employed the free software package «HIFU beam», developed at the Laboratory for Industrial and Medical Ultrasound (LIMU) of Moscow State University.[17, 18] This numerical toolbox allows for the modeling of axially symmetric focused acoustic fields based on the one-way form of the Westervelt equation. Real transducers, which only approximately satisfy axial symmetry, are modeled via an equivalent piston source: a spherical bowl of outer diameter *D*, central opening *d*, curvature radius *F*, and uniform normal particle velocity amplitude v_0 on the surface.

Equivalent-source parameters (*D*, *d*, *F*, and the effective surface pressure $p_0 = \rho_0 c_0 v_0$) are determined by fitting theoretical axial and focal-plane pressure profiles from the linear acoustic model to corresponding low-amplitude experimental measurements. From these fits, the ratio p_0/U_0 is also established, where U_0 is the drive voltage amplitude applied to the transducer

elements. Since the piezoelectric elements remain linear up to the manufacturer-specified continuous-wave limit of 10 V, nonlinear propagation at higher amplitudes is simulated by scaling p_0 proportionally with U_0.

C. ARRAY DESIGN AND ITS CHARACTERIZATION

Figure 1. Photo of 128-element focused ultrasound array used in the current study

The design and characteristics of the array were described in our previous publication [12] and are therefore presented here only briefly. The base of the array was an acrylic spherical bowl with a diameter of 500 mm and a radius of curvature of 500 mm (Fig. 1). The radiating elements of the array were 128 UP-3-01 piezoelectric transducers (OOO Aerofon, Volgograd, Russia) with a central frequency of 35.5 kHz each.[19] To suppress parasitic diffraction maxima, individual transducers were assembled into eight spirals with a shape ensuring a compact arrangement of the elements on the spherical base. The transducers were attached to the acrylic bowl using adjustable-length holders, which were tubes with external threads screwed into threaded holes in the base. Electrical wires powering the piezoelectric elements passed inside these tubes. The threads of the holders made it possible to adjust the position of the elements relative to the spherical cup with an accuracy of approximately 0.1 mm by screwing them in or out. Each holder, located on the rear (convex) side of the acrylic bowl, contained an audio jack, allowing the element to be connected to a power source. All array elements were electrically connected in parallel, so the array served as a single electrical load for the power source. A matching network consisting of appropriately selected reactive components (an inductor and a capacitor) was installed between the power amplifier and the antenna array. A 33120A signal generator (Agilent Technologies, USA) was used as the source of control signals fed to the input of the power amplifier. The signal from the generator was amplified using an AM 200 power amplifier (Atoll Electronique, Brecey, France), fed to the matching network, and then to the array.

To ensure effective focusing, the array elements were mutually phased so that the acoustic signals emitted by individual elements interfered constructively at the focal point. To achieve this, a microphone was placed at the array focus during setup, and individual elements sequentially emitted ultrasound at an operating frequency of 35.5 kHz. The microphone signal was monitored on an oscilloscope and compared with a reference signal at the same frequency. By adjusting the position of the element holders, the phase of the acoustic signal from the element and the reference signal was aligned.

The acoustic characteristics of the developed array were determined using transient acoustic holography.[20, 21] A hologram of the ultrasonic field was recorded using raster scanning and recording the acoustic signal at the nodes of a flat square grid with a pitch of 4 mm. A calibrated 46BE condenser microphone set (GRAS, Denmark) with a 1/4-inch diameter and a virtually linear amplitude-frequency response in the range of 0–100 kHz was used as the receiver. During the measurement, the microphone could be automatically moved to the desired position. A computer-

controlled micropositioning system (UMS-3, Precision Acoustics, UK) was used for this purpose. The hologram plane (scan plane) was perpendicular to the array axis and located at a distance from its center approximately equal to half the focal length. A grid size of 101×101 nodes was chosen, resulting in a scanning area of 400×400 mm. This allowed for full coverage of the beam's geometric dimensions. The center of the scanning area was located opposite the array center. During scanning, the microphone signal was recorded at each point on the hologram. The same electrical signal was applied to the array elements for each microphone position. This signal consisted of a 35.5 kHz tone pulse lasting 20 cycles with a smooth rise and fall of the envelope. To reduce noise, the signals were averaged over 16 repetitions in pulse-periodic mode. The repetition period was 10 ms. The microphone's electrical signal was recorded using a TDS5054B oscilloscope (Tektronix Inc., USA). The signal was recorded over a 4 ms time window, sufficient to measure the entire pulsed acoustic signal recorded by the microphone. The signal sampling rate was 1.6 μs per sample, corresponding to 2500 samples in the selected time window.

In addition to scanning the hologram (recording the two-dimensional structure of the acoustic field), measurements of the longitudinal distribution of the acoustic signal along the axis of the ultrasonic source and the transverse distribution in the focal plane were performed to control the focusing nature of the antenna array and determine the parameters of the equivalent piston source for use in modeling nonlinear effects. At the focal point, the microphone signal was additionally recorded at various excitation levels of the antenna array until the amplitude of the acoustic wave at the focal point reached the limit of the microphone's dynamic range of 160 dB.

D. USE OF A BROADBAND HYDROPHONE AS A MICROPHONE

Conventional microphones are not designed to receive high-amplitude ultrasonic signals. In addition to high acoustic pressure levels, which distort and saturate the microphone response, intense acoustic waves also exhibit a broad spectrum that extends beyond the sensitivity band of traditional microphones, as they undergo nonlinear distortion, including the formation of shock fronts. For example, the aforementioned GRAS condenser microphone set cannot receive signals with levels exceeding 160 dB and frequencies exceeding 100 kHz. Studying high-intensity acoustic waves in air requires specialized receivers. One possible approach is optical methods. For example, in Ref. 22, an optical interferometer was used to record shock waves from a spark source. This allowed the profile of a spherically diverging shock wave to be recorded with a resolution of 0.4 μs, which is almost an order of magnitude better than that of condenser microphones. Another method for recording broadband intense signals was described in a recent study, which used a ¼-inch-diameter cellular polypropylene film with metallized electrodes that was directly glued to the back plate of a commercially available condenser microphone cartridge.[11] This microphone allowed the reception bandwidth to be extended to 500 kHz, and the corresponding peak pressures reached 15 kPa. Another attractive possibility was proposed in the article,[23] in which a capsule hydrophone (HGL-0400, Onda Corporation, Sunnyvale, CA), originally designed for measurements in water, was employed as a microphone to record acoustic fields from an intense piezoelectric source with an operating frequency of 300 kHz and a 160 dB source pressure amplitude level. Because the operating frequency was quite high, close to the megahertz range for which the capsule hydrophone was originally designed, airborne ultrasound reception was not accompanied by significant distortion, allowing for the recording of a sawtooth wave generated by acoustic nonlinearity at some distance from the source. The measurement results were in good agreement with modeling using the Khokhlov-Zabolotskaya-Kuznetsov (KZK) equation.

In this study, we also used a capsule hydrophone as a microphone. It had a 0.2 mm diameter sensitive area (HGL-0200, Onda Corporation, Sunnyvale, CA). The difficulty of measuring low-

frequency ultrasound with such a receiver is that the frequencies are an order of magnitude lower than those used in Ref. 23, making the hydrophone's frequency response highly uneven due to reflections both within the hydrophone housing (where ultrasound absorption is low) and possible reflections from the hydrophone mounting device. Therefore, when recording fields from low-frequency ultrasonic emitters, the hydrophone, although a broadband receiver, significantly distorts the signal shape. The influence of frequency band irregularities due to multiple reflections could be compensated for by deconvolving the hydrophone's response using the amplitude-frequency response found by comparing the measured signal in shock-wave mode with the theoretical prediction based on modeling the nonlinear field from an equivalent piston radiator. We previously successfully used a similar approach to calibrate a capsule hydrophone in water [24]. An advantage of the capsule hydrophone is its wide bandwidth, up to 30 MHz and higher, which enables the reception of approximately a hundred harmonics and, thus, the correct recording of not only the smooth portion of the wave profile but also the shock fronts.

3. RESULTS

A. ACOUSTIC HOLOGRAPHY FOR RECONSTRUCTING THE SPATIAL FIELD STRUCTURE AND TRANSDUCER SURFACE VIBRATION

Figure 2 illustrates the acoustic hologram measurement setup and the resulting hologram, which consists of the two-dimensional amplitude and phase distributions of the acoustic field in a transverse plane intersected by the ultrasonic beam generated by the multi-element array under study. The beam is visibly confined to a central region well within the scanned area, confirming that the measurement aperture was sufficiently large to capture the entire hologram accurately.

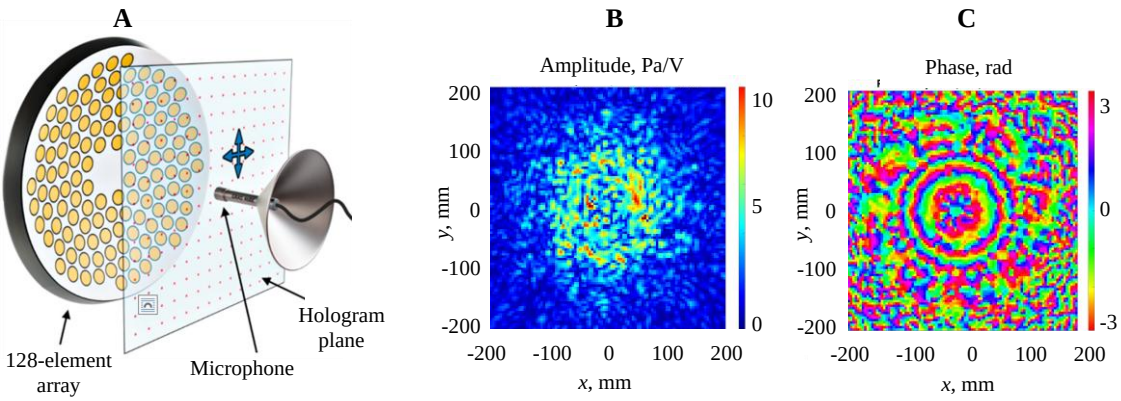

Figure 2. A) Experimental setup for recording a hologram. B) and C) Acoustic hologram – transverse distributions of amplitude (B) and phase (C) of acoustic pressure at a frequency of 35.5 kHz, measured at a distance of 200 mm in front of the focus. The pressure amplitude is indicated in Pa/V – it corresponds to the amplitude of the source voltage equal to 1 V.

Figure 3 presents the results of projecting the measured hologram onto two planes of practical interest. The top row shows the amplitude and phase distributions of the normal component of the surface vibration velocity reconstructed on a spherical surface that coincides with the radiating elements of the array. All individual transducers are clearly resolved. Only a few elements exhibit low vibration amplitude, which was later attributed to slight detuning of their resonance frequency

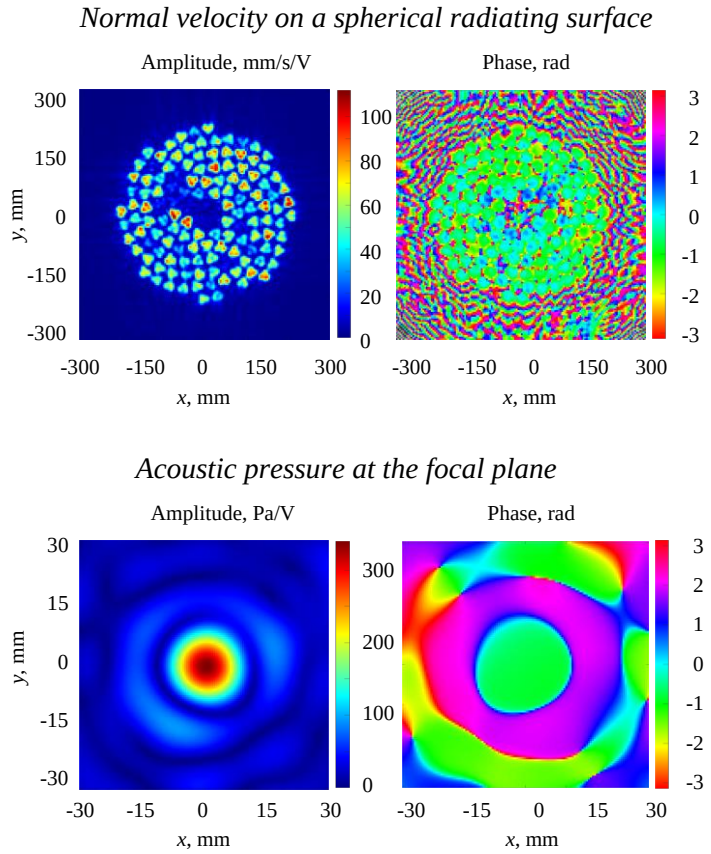

Figure 3. Projection of the measured hologram shown in Fig. 2 onto the array surface (top) and onto the focal plane (bottom).

Top: Amplitude and phase of the normal velocity distribution on the radiating surface. The amplitude is shown in mm/s per 1 V of electrical voltage applied to the array elements. Most of the elements appear clearly and radiate efficiently in sync with a phase of 0.

Bottom: Acoustic pressure distribution in the focal plane. The pressure amplitude is given in Pa/V - it corresponds to a source voltage amplitude of 1 V. Note that the image square is 30×30 mm, i.e. 10 times smaller than the size of the top images. The pressure amplitude is localized in a focal spot with a diameter close to the wavelength (~10 mm). The distribution is close to axisymmetric, indicating that the array can be approximated by an equivalent piston source (see also below).

from the operating frequency of 35.5 kHz. The phase distribution is highly uniform across the active elements, confirming coherent in-phase excitation and validating the mechanical alignment procedure used to align the transducers (fine adjustment by screwing/unscrewing the element holders within the acrylic support).

The bottom row in Fig. 3 shows the pressure amplitude and phase distributions in the intended focal plane. Within the displayed 30×30 mm region, nearly all acoustic energy is concentrated into a focal spot approximately 1 cm in diameter—close to the diffraction limit at this frequency and aperture size. Remarkably, the intensity distribution in the focal plane is nearly axially symmetric despite moderate non-uniformity of the source vibration amplitude. This high degree of axial symmetry allows the focal field to be accurately approximated by that of an ideal focused axisymmetric source in subsequent modeling.

B. DERIVING PARAMETERS OF AN EQUIVALENT FOCUSED PISTON SOURCE

To model the nonlinear focusing regime, the actual array is replaced by an idealized axisymmetric source: a uniformly vibrating spherical bowl with a central hole. The equivalent radiator parameters – focal length F, outer diameter D, and central hole diameter d – are obtained by fitting the linear-theory pressure distributions (along the axis and in the focal plane) to low-amplitude experimental data. Figure 4 compares the measured pressure distributions (dots) with the predictions of the optimized equivalent focused piston model (solid lines), using F = 484 mm, D = 455 mm, and d = 74 mm. The model shows good agreement with measurements throughout the entire field, particularly in the focal region – where pressure amplitude reaches its maximum and nonlinear effects become dominant at high drive levels. The small residual differences confirm that the equivalent uniformly vibrating spherical bowl accurately represents the linear focusing

properties of the real phased-array transducer. The measured focusing gain – defined as the ratio of the pressure amplitude at the geometric focus to the pressure amplitude on the radiating surface – was 33.5, yielding a linear intensity gain of 1122 (i.e., > 30 dB).

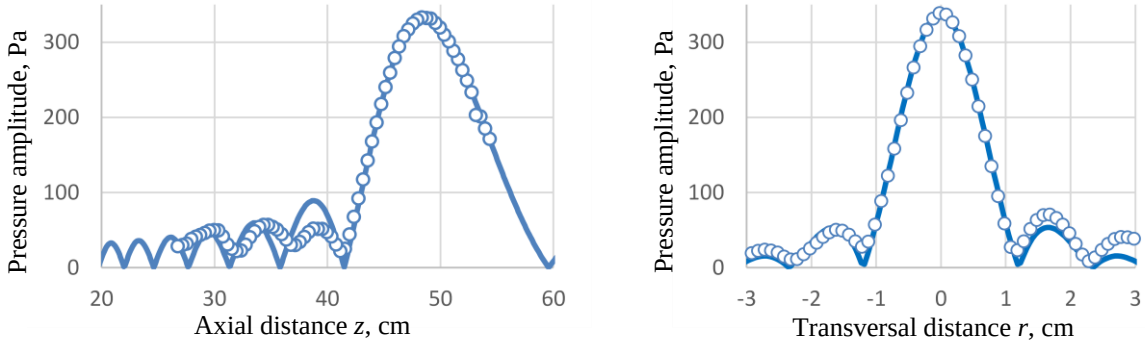

Figure 4. Pressure amplitude distribution along the acoustic axis (**left**) and in the focal plane perpendicular to the axis (**right**). Circles show microphone measurements; solid lines represent calculations performed with the equivalent focused-piston model.

C. HARMONIC AMPLITUDES AT THE FOCAL POINT: MEASUREMENTS AND NONLINEAR MODEL PREDICTIONS

In a separate experiment, the linear relationship between the voltage applied to the piezoelectric elements and the emitted acoustic pressure was verified and confirmed. Subsequently, taking into account the (unknown) sensitivity of the HGL hydrophone, the relationship between the effective surface pressure amplitude of the equivalent piston radiator $p_0 = \rho_0 c_0 v_0$ (where v_0 is the amplitude of the normal component of the surface vibration velocity) and the amplitude of the driving electrical voltage U_0 was established. The resulting calibration factor was p_0/U_0 = 17.3 Pa/V. This ratio was used to prescribe the source pressure amplitude p_0 from the known applied voltage U_0.

Since the absolute sensitivity of the HGL hydrophone was unknown, the nonlinear simulations were employed to determine it at the frequencies of the first four harmonics, where the signal-to-noise ratio was sufficiently high. In Figure 5, the circles show the measured amplitudes of the first four harmonics at the focus as a function of the source pressure amplitude p_0. The solid lines represent the results computed with the «HIFU Beam» program. The experimentally recorded harmonic amplitudes (originally in volts) were converted to pascals by matching them to the theoretical predictions. The resulting hydrophone sensitivities at the corresponding harmonic frequencies (35.5, 71, 106.5, and 142 kHz) were found to be 0.216, 0.166, 0.120, and 0.072 μV/Pa, respectively.

Remarkably, not only the absolute levels of the harmonic amplitudes (which are forced to match by the chosen sensitivity values), but also the detailed shape of their dependence on drive level, are in very close agreement between experiment and theory. This confirms the validity of representing the actual source field by the equivalent focused piston model.

Particularly noteworthy is the behavior of the fundamental harmonic: its attenuation at the focus relative to the linear-regime trend provides an unambiguous way to determine the true source pressure p_0 and, consequently, the absolute amplitudes of all harmonics at the focus. For example, at the maximum applied voltage of 11.3 V (corresponding to $p_0 \approx 200$ Pa), the focal pressure amplitude of the fundamental reaches 4400 Pa, corresponding to a sound pressure level of 167 dB re 20 μPa.

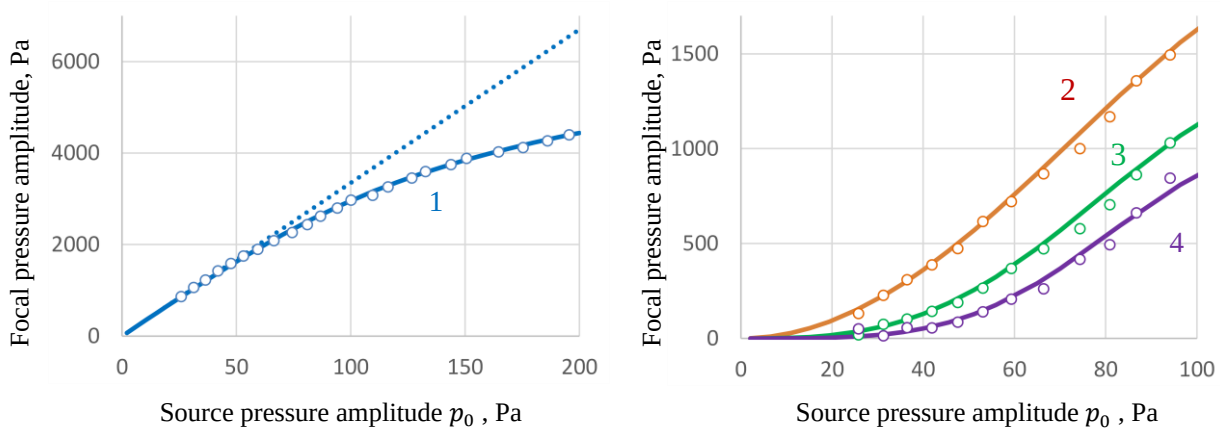

Figure 5. Harmonic pressure amplitudes at the geometric focus as a function of the effective surface pressure amplitude p_0 of the equivalent focused piston. Solid lines – nonlinear model predictions; circles – experimental measurements. **Left:** fundamental (1st) harmonic; the dotted line indicates the linear-regime prediction. **Right:** 2nd, 3rd, and 4th harmonics (harmonic order labeled next to each curve).

D. ACOUSTIC WAVEFORM AT THE FOCUS AND MEASUREMENT OF THE SHOCK FRONT RISE TIME

Along with the behavior of harmonic amplitudes, the nonlinear distortion of the waveform and, in particular, the formation of shock fronts are of significant interest. Modeling based on the Westervelt equation, implemented in the «HIFU beam» software, demonstrates that the multi-element transducer used in the experiment enabled strongly nonlinear regimes to be achieved – i.e., it truly behaved analogously to megahertz-range HIFU transducers. Note that in the simulations, frequency-dependent absorption in air was calculated using the standard atmosphere model, taking into account the temperature and humidity measured during the experiment.[25, 26]

Figure 6 shows a characteristic waveform at the focus in the strongly nonlinear regime. The experimental signal was acquired using the HGL microphone-hydrophone, which is capable of

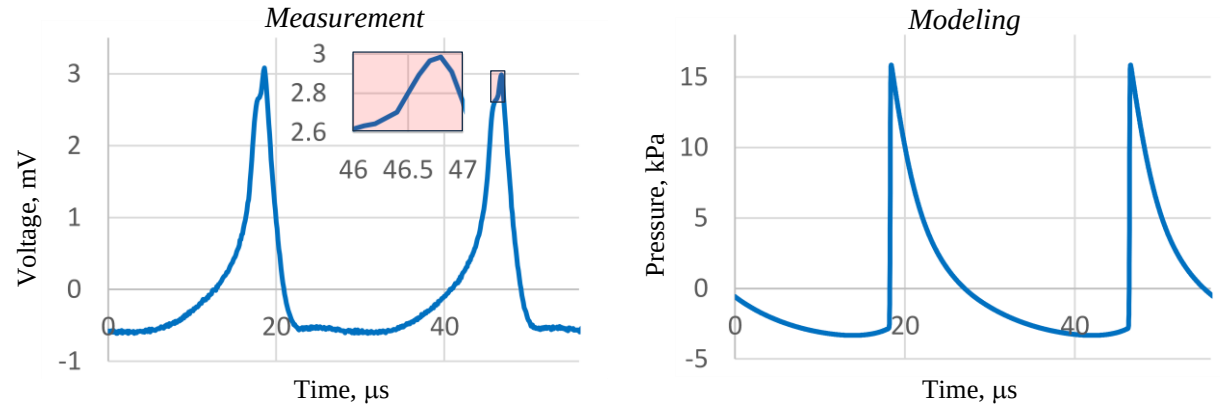

Figure 6. Two periods of the acoustic pressure waveform at the focus, obtained at a transducer drive voltage amplitude of 11.3 V (corresponding to a pressure amplitude of an equivalent piston radiator $p_0 \approx 200$ Pa). **Left:** Experimental signal recorded with the HGL fiber-optic hydrophone. **Right**: Results of numerical modeling. The experimental waveform deviates from the theoretical prediction primarily due to the nonuniform frequency response of the hydrophone's sensitivity. Despite this, the shock front is clearly visible as a sharp discontinuity at the waveform peak. An enlarged view of the shock front is provided in the inset.

recording signals over a broad bandwidth and does not suffer from amplitude saturation – unlike the GRAS microphone set. Due to the nonuniform frequency dependence of its sensitivity, the HGL sensor distorts the smooth portions of the waveform. Nevertheless, it clearly captures the presence of a shock in the wave profile. This shocked region is shown enlarged in the inset. The duration of the shock transition is approximately 0.2 μs, indicating that the HGL sensor is able to resolve relatively short shock fronts.

It should also be noted, based on the modeling results, that the peak positive pressure at the focus reached 15.8 kPa, corresponding to 178 dB. This level is comparable to, and even exceeds, the amplitudes typically achieved in commercial high-intensity ultrasound systems.[3]

4. CONCLUSIONS

The development of high-intensity focused ultrasound (HIFU) transducers operating in air at low ultrasonic frequencies presents a challenging and fascinating task, both for a wide range of potential applications and for fundamental studies of nonlinear effects in tightly focused high-intensity acoustic beams. This paper describes one such system developed at the Laboratory for Industrial and Medical Ultrasound (LIMU), Moscow State University. The array comprises 128 piezoelectric transducers mounted on a spherical support, with individual positioning adjustment of each element. The operating frequency is 35.5 kHz, and both the aperture diameter and the geometric focal length are 0.5 m. Waveform measurements were performed using a non-conventional microphone – specifically, a receiver based on a hydrophone originally designed for the megahertz frequency range (HGL-0200). It is demonstrated that this sensor remains fully capable of accurately detecting signals at these much lower frequencies. The measured dependence of harmonic amplitudes on the driving voltage amplitude enabled simultaneous calibration of both the receiver sensitivity at the frequencies of interest and the electroacoustic conversion efficiency (voltage-to-pressure) of the transducer itself. Measurements showed that shock fronts develop in the focal waveform, with peak positive acoustic pressure levels exceeding 175 dB (re 20 μPa).

The experimental investigation of airborne HIFU was complemented by numerical modeling based on the Westervelt equation. Simulations were performed using the «HIFU beam» free software package developed at LIMU. The boundary condition at the transducer surface was specified using an equivalent piston source model, with parameters derived from microphone measurements of the focal region pressure field. Additionally, acoustic holography was applied to characterize the multi-element array and the radiated sound field. The results confirm that the system successfully generates shock-wave regimes in air. All observed effects and quantitative values match the numerical predictions very closely when the boundary conditions are taken from the experimental calibration.

ACKNOWLEDGMENTS

This work was supported by the Russian Science Foundation (grant no. 25-12-00141).

REFERENCES

1. M.R. Bailey, V.A. Khokhlova, O.A. Sapozhnikov, S.G. Kargl, and L.A. Crum, “Physical mechanisms of the therapeutic effect of ultrasound (a review),” Acoust. Phys. **49**(4), 369–388 (2003). https://doi.org/10.1134/1.1591291

2. O.A. Sapozhnikov, V.A. Khokhlova, R.O. Cleveland, P. Blanc-Benon, M.F. Hamilton, "Nonlinear acoustics today," Acoust. Today **15**(3), 55–64 (2019). https://doi.org/10.1121/AT.2019.15.3.55

3. J.A. Gallego-Juarez, K.F. Graff, M. Lucas, *Power Ultrasonics* (Woodhead Publishing, 2023, 896 p.)

4. C.M.G. Charoux, K.S. Ojha, C.P. O'Donnell, A. Cardoni, B.K. Tiwari, "Applications of airborne ultrasonic technology in the food industry," J. Food Eng. **208**, 28–36 (2017). https://doi.org/10.1016/j.jfoodeng.2017.03.030

5. J.A. Gallego-Juarez, "High-power ultrasonic processing: Recent developments and prospective advances," Phys. Procedia **3**(1), 35–47 (2010). https://doi.org/10.1016/j.phpro.2010.01.006

6. A. Marzo, A. Barnes, and B.W. Drinkwater, "TinyLev: A multi-emitter single-axis acoustic levitator," Rev. Sci. Instrum. **88**, 085105 (2017). https://doi.org/10.1063/1.4989995

7. A. Marzo, M. Caleap, and B.W. Drinkwater, "Acoustic virtual vortices with tunable orbital angular momentum for trapping of Mie particles," Phys. Rev. Lett. **120**(4), 044301 (2018). https://doi.org/10.1103/PhysRevLett.120.044301

8. A. Marzo, S.A. Seah, B.W. Drinkwater, D.R. Sahoo, B. Long, S. Subramanian, "Holographic acoustic elements for manipulation of levitated objects," Nat. Commun. **6**(1), 8661 (2015). https://doi.org/10.1103/PhysRevLett.120.044301

9. R.W. Haupt, "High-powered parametric acoustic array in air," J. Acoust. Soc. Am. **125**(4), 2688–2688 (2009). https://doi.org/10.1121/1.4784274

10. M. Liebler, C. Kling, A. Gerlach, and C. Koch, "Experimental characterization of high-intensity focused airborne ultrasound fields," J. Acoust. Soc. Am. **148**(3), 1713–1722 (2020). https://doi.org/10.1121/10.0001974

11. T. Kamakura, S. Sakai, H. Hayashi, Y. Yasuno, and H. Nomura, "Cartridge-type cellular polypropylene microphone with broadband sensitivity," Acoustical Science and Technology, e25–e21 (2025). https://doi.org/10.1250/ast.e25.21

12. S.A. Asfandiyarov, S.A. Tsysar, and O.A. Sapozhnikov, "A multielement low-frequency ultrasonic transducer as a source of high-intensity focused ultrasound in air," Acoust. Phys. 2024. V. 70. № 4. P. 759–768. https://doi.org/10.1134/S1063771024601936

13. P. Westervelt, "Parametric acoustic array," J. Acoust. Soc. Am. **35**(4), 535–537 (1965). https://doi.org/10.1121/1.1918525

14. H.E. Bass, L.C. Sutherland, J. Piercy, and L. Evans, "Absorption of sound by the atmosphere," In: Physical acoustics: Principles and methods. v. 17 (A85-28596 12–71). Orlando, 17, pp.145–232 (1984).

15. C.J. Moen, "Ultrasonic absorption in liquids," J. Acoust. Soc. Am., 1951, **23**(1), pp. 62–70. https://doi.org/10.1121/1.1906730

16. W. Kreider, P.V. Yuldashev, O.A. Sapozhnikov, N. Farr, A. Partanen, M.R. Bailey, and V.A. Khokhlova, "Characterization of a multi-element clinical HIFU system using acoustic holography and nonlinear modeling," // IEEE Transactions on Ultrasonics, Ferroelectrics, and Frequency Control, 2013, **60**(8), pp.1683–1698. https://doi.org/10.1109/TUFFC.2013.2750

17. P.V. Yuldashev, I.S. Mezdrokhin, and V.A. Khokhlova, "Wide-angle parabolic approximation for modeling high-intensity fields from strongly focused ultrasound transducers," Acoust. Phys. **64**(3), 309–319 (2018). https://doi.org/10.1134/S1063771018030168

18. P.V. Yuldashev, M.M. Karzova, W. Kreider, P.B. Rosnitskiy, O.A. Sapozhnikov, and V.A. Khokhlova, "«HIFU Beam»: A simulator for predicting axially symmetric nonlinear acoustic fields generated by focused transducers in a layered medium," // IEEE Trans. Ultrason., Ferroelect., Freq. Contr. **68**(9), 2837–2852 (2021). https://doi.org/10.1109/TUFFC.2021.3074611

19. A.F. Geyer and V.A. Ponomarev, "Development of piezoceramic electroacoustic transducers for acoustic devices with a sound pressure of 125 dB and more," Voprosy Radioelektroniki, no. 10, 11–16 (2019). [in Russian]

20. O.A. Sapozhnikov, A.E. Ponomarev, and M.A. Smagin, "Transient acoustic holography for reconstructing the particle velocity of the surface of an acoustic transducer," Acoust. Phys. **52**(3), 324–330 (2006). https://doi.org/10.1134/S1063771006030134

21. O.A. Sapozhnikov, S.A. Tsysar, V.A. Khokhlova, and W. Kreider, "Acoustic holography as a metrological tool for characterizing medical ultrasound sources and fields," J. Acoust. Soc. Am. **138**(3), 1515–1532 (2015). https://doi.org/10.1121/1.4928396

22. P. Yuldashev, M. Karzova, V. Khokhlova, S. Ollivier, and P. Blanc-Benon, "Mach-Zehnder interferometry method for acoustic shock wave measurements in air and broadband calibration of microphones," J. Acoust. Soc. Am. **137**(6), 3314–3324 (2015). https://doi.org/10.1121/1.4921549

23. E. Vatankhah, Y. Meng, Z. Liu, X. Niu, and N.A. Hall, "Characterization of high intensity progressive ultrasound beams in air at 300 kHz," J. Acoust. Soc. Am. **153**(5), 2878–2878 (2023). https://doi.org/10.1121/10.0019376

24. O.A. Sapozhnikov, V.A. Khokhlova, and D. Cathignol, "Nonlinear waveform distortion and shock formation in the near field of a continuous wave piston source," J. Acoust. Soc. Am. **115**(5), 1982–1987 (2004). https://doi.org/10.1121/1.1695433

25. Standard, I.S.O., 1993. *Acoustics – Attenuation of sound during propagation outdoors – Part 1: Calculation of the absorption of sound by absorption by the atmosphere*.

26. H.E. Bass, L.C. Sutherland, A.J. Zuckerwar, D.T. Blackstock, and D.M. Hester, "Atmospheric absorption of sound: Further developments," J. Acoust. Soc. Am. **97**(1), 680–683 (1995). https://hdl.handle.net/10945/62134